ORIGINAL RESEARCH

A dedicated paediatric [18F]FDG PET/CT dosage regimen

Christina P. W. Cox[*], Daniëlle M. E. van Assema, Frederik A. Verburg, Tessa Brabander, Mark Konijnenberg and Marcel Segbers

Abstract

Background: The role of 2-[18F]fluoro-2-deoxy-D-glucose ([18F]FDG) positron emission tomography/computed tomography (PET/CT) in children is still expanding. Dedicated paediatric dosage regimens are needed to keep the radiation dose as low as reasonably achievable and reduce the risk of radiation-induced carcinogenesis. The aim of this study is to investigate the relation between patient-dependent parameters and [18F]FDG PET image quality in order to propose a dedicated paediatric dose regimen.

Methods: In this retrospective analysis, 102 children and 85 adults were included that underwent a diagnostic [18F]FDG PET/CT scan. The image quality of the PET scans was measured by the signal-to-noise ratio (SNR) in the liver. The SNR liver was normalized (SNRnorm) for administered activity and acquisition time to apply curve fitting with body weight, body length, body mass index, body weight/body length and body surface area. Curve fitting was performed with two power fits, a nonlinear two-parameter model $\alpha\, p^{-d}$ and a linear single-parameter model $\alpha\, p^{-0.5}$. The fit parameters of the preferred model were combined with a user preferred SNR to obtain at least moderate or good image quality for the dosage regimen proposal.

Results: Body weight demonstrated the highest coefficient of determination for the nonlinear ($R^2 = 0.81$) and linear ($R^2 = 0.80$) models. The nonlinear model was preferred by the Akaike's corrected information criterion. We decided to use a SNR of 6.5, based on the expert opinion of three nuclear medicine physicians. Comparison with the quadratic adult protocol confirmed the need for different dosage regimens for both patient groups. In this study, the amount of administered activity can be considerably reduced in comparison with the current paediatric guidelines.

Conclusion: Body weight has the strongest relation with [18F]FDG PET image quality in children. The proposed nonlinear dosage regimen based on body mass will provide a constant and clinical sufficient image quality with a significant reduction of the effective dose compared to the current guidelines. A dedicated paediatric dosage regimen is necessary, as a universal dosing regimen for paediatric and adult is not feasible.

Keywords: Image quality, PET, [18F]FDG activity, Dose optimization, Patient size, Body weight

Background

Currently, the role of 2-[18F]fluoro-2-deoxy-D-glucose ([18F]FDG) positron emission tomography/computed tomography (PET/CT) imaging is still expanding in the diagnosis and follow-up of paediatric oncologic, infectious and inflammatory diseases [1, 2]. This expansion brings a point of concern, since both the CT and the [18F]FDG expose patients to ionizing radiation, which can cause radiation-induced effects later in life [3]. The risk of radiation-induced carcinogenesis is higher in children, as they have a longer post-radiation exposure life expectancy compared to adults [3]. To reduce this risk, the radiation dose of paediatric PET/CT scans should be as low as reasonably achievable

*Correspondence: c.cox@erasmusmc.nl
Department of Radiology & Nuclear Medicine, Erasmus Medical Center, Postbus, 2040 3000 CA Rotterdam, The Netherlands

Cox *et al. EJNMMI Res*   (2021) 11:65

Page 2 of 10

(ALARA) [4] with acceptable image quality and within a reasonable acquisition time. Therefore, optimization and harmonization of paediatric PET/CT imaging protocols are essential [5].

For performing paediatric nuclear medicine procedures, both the Society of Nuclear Medicine and Molecular Imaging (SNMMI) and European Association of Nuclear Medicine (EANM) recommend the EANM paediatric dosage card (version 5.7.2016) [6, 7] or the 2016 North American Consensus guidelines (NACG) [7, 8]. Both these guidelines have, however, several shortcomings as they are derived from adult-based protocols [9–12], and both focus on radiation dose without taking image quality into account [9–13]. Moreover, the EANM paediatric dosage card recommends even higher administered activities per kilogram than the adult 2015 EANM [18F]FDG guidelines [14]. The optimized adult guidelines recommend a quadratic dosage regimen based on body mass to obtain sufficient constant image quality, which was reported by a study of de Groot et al. [15] using signal-to-noise ratio as a surrogate for image quality. This study investigated the relationship between a patient-dependent parameter, for example, body mass, BMI, LBM, fat mass (defined by body mass minus the lean body mass) and body mass per body/length and the administered [18F]FDG. Another option is to use a linear dosage regimen < 75 kg and a quadratic dosage regimen > 75 kg to compensate for the lower signal-to-noise ratio due to excessive attenuation in heavier patients. Optimizing image quality in these patients was investigated by several studies [16–20].

In contrast to adult dose regimens, only a few studies have been published on optimizing administered activities in children. Accorsi et al. [10] found that weight was the best patient-dependent indicator for the administered activity necessary to obtain constant sufficient image quality. A pilot study of van Gent et al.[21] focussed on body weight showed that a linear relationship between body weight and administered activity results in a constant image quality. Other studies have reduced the administered [18F]FDG activity per kilogram of body weight based on simulations of PET low-dose scans by reduction of count rates [11, 22, 23].

The Paediatric Dosage Harmonization Working Group and the 2020 paediatric guideline stated that more data are needed for evidence-based optimisation of the current guidelines [7, 24]. This can be achieved by dedicated paediatric studies, based on the methods used for the adult guidelines, for different PET systems and reconstruction methods to provide the needed data for updating the paediatric guidelines. The aim of this study, therefore, is to investigate the relation between patient-dependent parameters and [18F]FDG PET image quality and to propose a dedicated paediatric dose regimen that provides a constant and clinical sufficient image quality.

Methods

Patients

This retrospective study consecutively included 102 children (54 boys and 48 girls; mean age 12.5 ± 4.6 years; range 0.5–17.9 years) that underwent a diagnostic [18F]FDG PET/CT scan at the Erasmus Medical Centre between January 2017 and July 2020. Inclusion criteria were: preparation according to local protocol; serum glucose < 7.0 mmol/L; administered activity $\pm 10\%$ of the recommended activity; PET acquisition time 60 ± 5 min post-injection; and when disease was present no signs of extensive liver involvement on PET images. The same criteria were used to select 85 adult patients (26 male and 59 female; mean age 57.0 ± 16.5 years; range 22.0–83.0) with as much as possible the same body weight distribution to compare with the paediatric results. The study was approved by the Medical Ethical Committee of the Erasmus Medical Centre (MEC-2021–0078), and procedures were in accordance with the Declaration of Helsinki of 1964, as revised in 2013.

Patient-dependent parameters

For each patient, the patient-dependent parameters were collected or calculated in order to investigate the relationship between these parameters and [18F]FDG PET image quality. Body weight (BW) [kg] and body height (H) [m] were collected from the patient files. Body mass index (BMI), body weight per body height (BWH) and body surface area (BSA) were calculated as follows [25]:

$$\text{Body mass index (BMI)} := \frac{M}{H^2} (\text{kg/m}^2)$$

$$\text{Body weight per body height(BWH)} := \frac{M}{H} (\text{kg/m})$$

$$\text{Body surface area (BSA)} := 0.007184 \times M^{0.425} \times H^{0.725} (\text{m}^2)$$

[18F]FDG PET/CT

Patients were prepared according to local protocols for [18F]FDG PET/CT in children and adults. Children had to fast for four hours prior to injection and were stimulated to drink water (body weight $\times$ 10 ml < 10 years or 500–1000 ml > 10 years) during the last two hours before injection. Adults had to fast for six hours and drink 1000 ml of water before injection. Additionally, 17 children and 10 adults followed a carbohydrate-restricted diet for 24 h and fasted the last 12 h to suppress myocardial [18F]FDG uptake. Uptake of [18F]FDG in brown

Cox *et al. EJNMMI Res* (2021) 11:65

Page 3 of 10

adipose tissue was suppressed in 91 children and 17 adults by administering Propranolol (0.33 mg [mg] x BW with a maximum of 20 mg one hour before the injection for children and a fixed dose of 20 mg for adults. Dosing of [18F]FDG activity was determined with the local linearized quadratic dose regimen of 1.7 megabequerel per kilogram (MBq/kg) ($\leq$ 55 kg, 68 children, with a minimum of 14 MBq; 36 adults); 2.3 MBq/kg (55-70 kg, 26 children; 29 adults); 3.0 MBq/kg (71–95 kg, 7 children; 10 adults); and 4.0 MBq/kg ($\geq$ 96 kg, 1 child; 10 adults) and was intravenously injected (children median: 82 MBq; range 13–392 MBq and adults median: 138 MBq; range 56–532 MBq) followed by resting in a warm and quiet room. PET images were acquired 60 ± 5 min for children and 59 ± 3 min for adults after tracer injection in supine position on a Siemens Biograph mCT PET/CT scanner (Siemens Healthineers, Erlangen, Germany). According to our local scan protocol, first a whole-body low-dose CT with optimized parameters [26–28] was acquired for attenuation correction and localization purposes (Teenager/adult values in brackets). 80 kV (120 kV); Quality reference mAs 140 (40 mAs); automatic exposure control strength strong (average); rotation time 0.5 s; pitch 0.8 mm; slice thickness 2 mm (3 mm); reconstructed slice thickness 2 mm (3 mm); and a Siemens B19f low-dose for emission computed tomography kernel. Directly after the low-dose CT, PET acquisition started with an acquisition time of 3 min per bed position (mbp) from the inguinal region to the skull base with the arms up (61 children and all adults). Another 41 children (31 arms up, 10 arms down) were scanned from the skull base to the feet with 2 mbp for the additional lower extremities. Once acquisition was finished, PET scans were corrected for scatter and attenuation using the low-dose CT, followed by reconstruction using ordered subset expectation maximization (OSEM; 3 iterations; 21 subsets; point spread function (PSF) recovery; time of flight (TOF); a 3 mm Gaussian post-reconstruction filter on a matrix of 200×200 with a pixel size of 4.1×4.1 mm and 3 mm slice thickness.

Image analysis

The reconstructed PET scans were analysed for image quality based on the approach as described by de Groot et al. [15] and previously used by Cox et al. [29]. Image quality was measured with the signal-to-noise ratio (SNR) in the liver. To determine the SNR liver, a volume of interest (VOI) was placed in a lesion-free homogeneous part of the right liver lobe (diameter 3 cm) using Hermes Hybrid viewer 2.6D software (Hermes Medical Solutions, Stockholm, Sweden). The VOIs were placed at least 1 cm from the edge of the liver to avoid partial volume effects. The SNR liver was calculated by dividing the liver standard uptake value (SUV) mean normalized for body weight (SUVbw) by the standard deviation (SD) [15]. The liver SUVmean can also be used as a measure for liver deoxyglucose metabolism [30, 31]. In order to compare the liver deoxyglucose metabolism between children and adults, the liver SUVmean normalized by body surface area (SUVbsa) was determined. This value is less dependent on body size and age compared to SUVbw and therefore a better value for liver deoxyglucose metabolism [30, 31].

PET image quality depends on the time per bed position and the amount of administered activity. The product of these parameters is the dose time product (DTP [MBq·min]). The SNR liver can be normalized (SNRnorm liver [(MBq·min)$^{-1/2}$]) for the administered activity and scan time per bed position by assuming Poisson statistics in which noise increases with the square root of the signal [15]. The SNRnorm liver is assumed independent of scan time and administered activity.

$$\text{SNRnorm liver} = \frac{\text{SNR liver}}{\sqrt{\text{DTP}}} \tag{1}$$

Statistical analysis

All statistical analyses were performed using Graphpad PRISM version 9. In order to test for significant differences in liver deoxyglucose metabolism (liver SUVmean) and image quality (SNR liver and SNRnorm liver) between children and adults, an unpaired t-test ($\alpha = 0.05$) or a Mann–Whitney U test ($\alpha = 0.05$) after testing the data for normality by a Shapiro–Wilk test ($\alpha = 0.05$) was performed. Furthermore, a Pearson product correlation was run to determine the correlations between SNR liver and SNRnorm liver with age in both patient groups.

The coefficient of determination (Pearson R^2) was used to select the best patient-dependent parameter after curve fitting of each parameter with SNRnorm liver. Curve fitting was applied to the parameters by using a power function (Eq. 2) to obtain a nonlinear dosage regimen as described before by the Groot et al. [15]:

$$\text{SNR}_{\text{norm liver, fit}} = \alpha p^{-d}, \tag{2}$$

where α and d are fit parameters and p is the patient-dependent parameter.

Curve fitting was also performed with Eq. 3 to obtain a linear dosage regimen:

$$\text{SNR}_{\text{norm liver, fit}} = \alpha p^{-0.5}, \tag{3}$$

where α is the fit parameter and p is the patient-dependent parameter.

Cox *et al. EJNMMI Res* (2021) 11:65

Page 4 of 10

Preference between the two models for each patient-dependent parameter was determined by the difference between the Akaike's corrected information criterion values (ΔAICc) [32].

To determine significant differences between the patient-dependent parameter fit with the highest R^2 and the other patient-dependent parameters fits, the relative error between SNRnorm liver and SNRfit liver was calculated for each data point using (SNRfit liver − SNRnorm liver)/SNRfit liver × 100%. The relative error between the fits was tested with one-way ANOVA test ($\alpha = 0.05$) or a nonparametric Friedman test with additional post hoc tests after testing for normality [15].

The fit parameters of the best patient-dependent parameter were used for the dose regimen proposal. The fit parameters were entered in the following expressions:

Combining Eq. 1 and 2 results in the following non-linear expression for the DTP [MBq·min] [15]:

$$\text{DTP} = \frac{\text{SNR liver}^2}{\alpha^2} \times p^{2d}. \tag{4}$$

In the linear dosage regimen (d = 0.5), DTP [MBq·min] is indicated by the following linear expression:

Table 1 Paediatric patient-dependent parameters and SUV values

Parameters	Mean ± SD	Range	Median
Body weight (kg)	45.9 ± 19.9	3.8–96.0	46.5
Body height (m)	1.49 ± 0.26	0.57–1.86	1.58
BMI (kg/m^2)	19.4 ± 4.3	11.7–33.9	18.8
BWH (kg/m)	29.6 ± 9.9	6.7–55.2	29.6
BSA (m^2)	1.5 ± 0.5	0.3–2.5	1.7

$$\text{DTP} = \frac{\text{SNR liver}^2}{\alpha^2} \times p. \tag{5}$$

Results

Patient-dependent parameters

The measurements and calculations of the paediatric patient-dependent parameters are displayed in Table 1.

Liver deoxyglucose metabolism

An unpaired t-test was performed to compare the liver deoxyglucose metabolism between children and adults. This showed that SUVbsa in children (0.57 ± 0.10) was significant lower (t (185) = 7.82, $p < 0.001$) compared with SUVbsa in adults (0.69 ± 0.10) with a mean difference of 0.11 (95%CI, 0.09 to 0.14).

Image quality

To compare the SNR liver between children and adults an unpaired T-test was performed, which showed a significant (t (185) = 4.561, $p < 0.001$) difference in mean SNR liver between children (6.1 ± 0.9) and adults (6.7 ± 0.7). Also, the Mann–Whitney U test to compare the mean SNRnorm liver between adults (0.34 ± 0.10) and children (0.41 ± 0.15) revealed a significant ($U = 3087$, $p < 0.001$) difference between these two groups as displayed in Fig. 1. In children, the correlation between SNR liver and age showed a weak significant positive correlation ($r = 0.272$, $n = 102$, $p = 0.006$). For adults, both SNR liver and SNRnorm liver showed no correlations with age of, respectively, $r = -0.138$, $n = 85$, $p = 0.208$ and $r = -0.092$, $n = 85$, $p = 0.400$. This is in contrast to SNRnorm liver in children, which strongly correlated with age in a negative direction ($r = -0.795$, $n = 102$, $p < 0.001$).
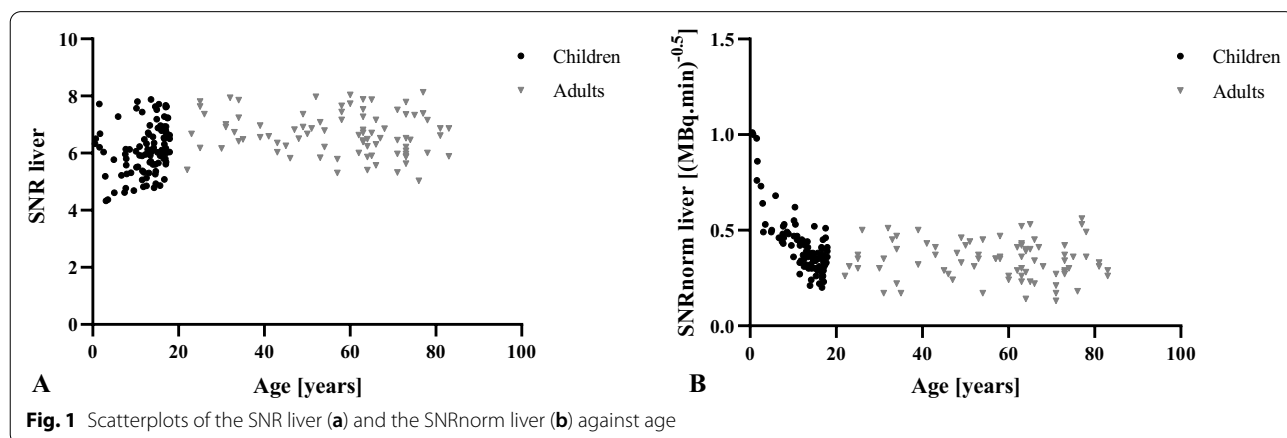

Fig. 1 Scatterplots of the SNR liver (**a**) and the SNRnorm liver (**b**) against age

Cox *et al. EJNMMI Res*   (2021) 11:65

Page 5 of 10

Curve fitting

The results of the curve fitting of SNRnorm liver with patient-dependent parameters are presented in Fig. 2 and Table 2. As can be seen body weight shows for both curves the highest R^2 (0.81 and 0.80, respectively). The nonlinear model is the preferred model, according to the AICc. For this model, the Friedman test with additional Dunn–Bonferroni post hoc test revealed only a significant difference ($p < 0.05$) between the fit of body weight and the fit of body height. (Table 2).
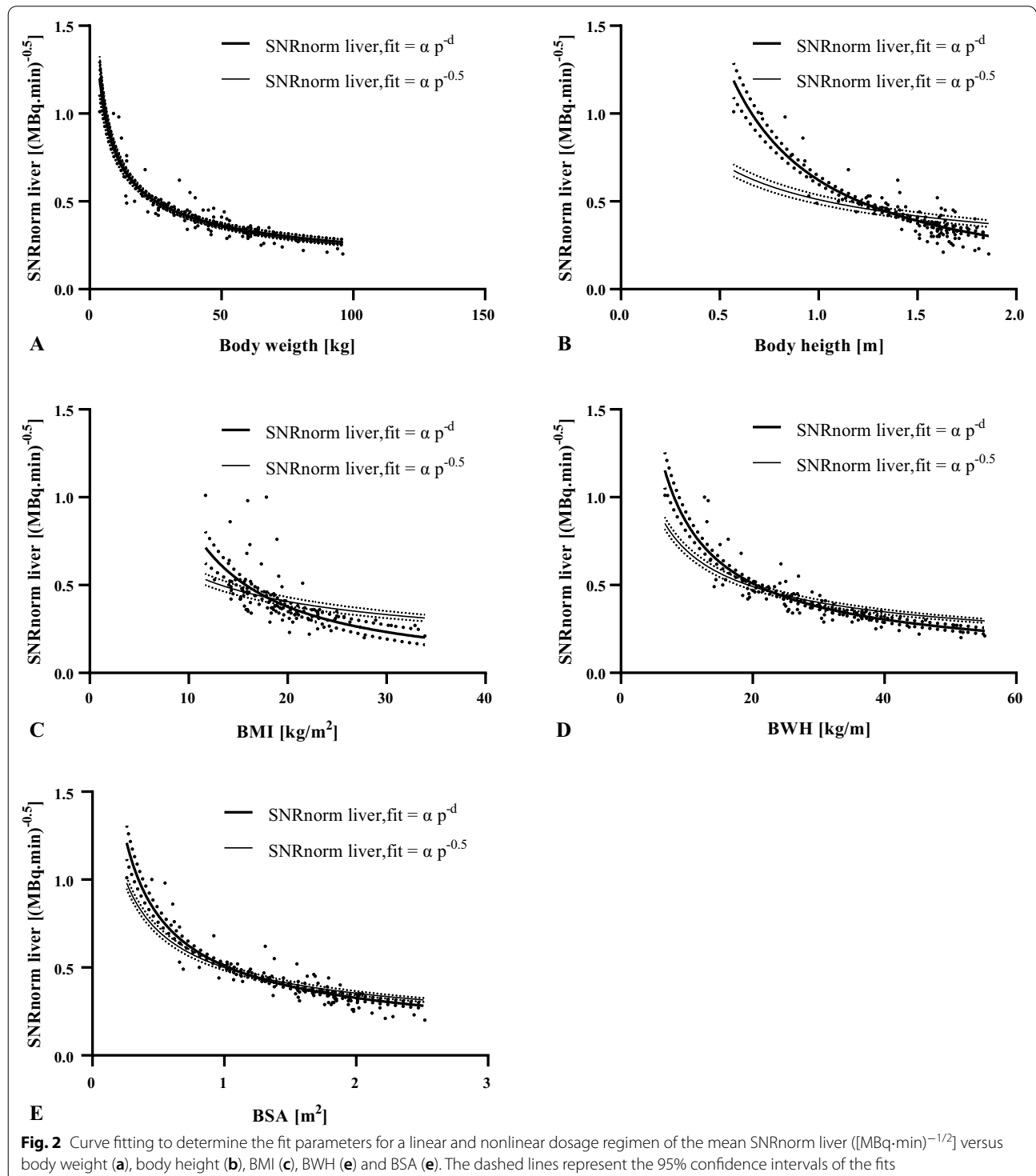

Fig. 2 Curve fitting to determine the fit parameters for a linear and nonlinear dosage regimen of the mean SNRnorm liver ([MBq·min]$^{-1/2}$) versus body weight (**a**), body height (**b**), BMI (**c**), BWH (**e**) and BSA (**e**). The dashed lines represent the 95% confidence intervals of the fits

Cox *et al. EJNMMI Res* (2021) 11:65

Page 6 of 10

Table 2 Fits of SNRnorm liver with the patient-dependent parameters

Patient-dependent parameters	SNRnorm liver, fit = α p$^{-0.5}$			SNRnorm liver, fit = α p^{-d}					
	α	R^2	*p* value	α	d	R^2	*p* value	ΔAICc	AIC%
Body weight (kg)	2.51	0.80	-	2.23	0.46	0.81	-	1.86	23.8 vs 71.20
Body height (m)	0.51	0.47	< 0.001	0.62	1.15	0.78	0.046	88.44	< 0.01 vs > 99.99
BMI (kg/m^2)	1.82	0.27	< 0.001	13.26	1.19	0.41	> 0.999	18.29	0.01 vs 99.99
BWH (kg/m)	2.20	0.67	< 0.001	4.73	0.74	0.78	> 0.999	33.61	< 0.01 vs > 99.99
BSA (m^2)	0.50	0.75	0.001	0.51	0.64	0.81	0.085	23.89	< 0.01 vs > 99.99

The SNR value for the proposed dosage regimen was set to 6.5. This value was based on an internal adult analysis concerning the shift form a linearized quadratic dosage regimen to a quadratic dosage regimen. This analysis showed that an SNR of 6.5 revealed satisfactory image quality for our nuclear medicine physicians. Thus, children showed a lower mean SNR compared to adults and the nuclear medicine physicians experienced sometimes scans with a poor image quality in children < 20 kg. Therefore, three nuclear medicine physicians decided to equalize these values and use an SNR of 6.5 for both dosage regimens.

The proposed dedicated dosage regimen was obtained by combining Eq. 4 with an SNR liver of 6.5 and the fit parameters of body mass which are α = 2.23 (95% CI 1.90 to 2.51) and d = 0.46 (95% CI 0.43 to 0.50). This resulted in the following nonlinear expression for the DTP [MBq·min] with a minimum of 26 MBq conform the guidelines [7]:

$$DTP = 8.5 \times M^{0.92}. \qquad (6)$$

Comparison of the proposed dosage regimen with the adult dosage regimen and the current paediatric dosage regimen in guidelines.

Figure 3 shows the fits of SNRnorm liver versus body weight that corresponds to the proposed nonlinear paediatric dosage regimen and the new Erasmus MC quadratic dosage regimen for adults. It can be seen that the nonlinear dosage regimen fits perfectly for children (Fig. 3a) and not for adults (Fig. 3b), whereas a quadratic dosage regimen fits perfectly for adults and not for children. No universal dose regimen could be found for children and adults together neither nonlinear nor quadratic (Fig. 3c).

In Fig. 4, our dosage regimens with an acquisition time of 3 mbp are compared with those of the EANM and NACG guidelines. As can be seen our new dosage regimen (65 MBq and 3.6 mSv [33]) will reduce the amount of administered activity and radiation dose with
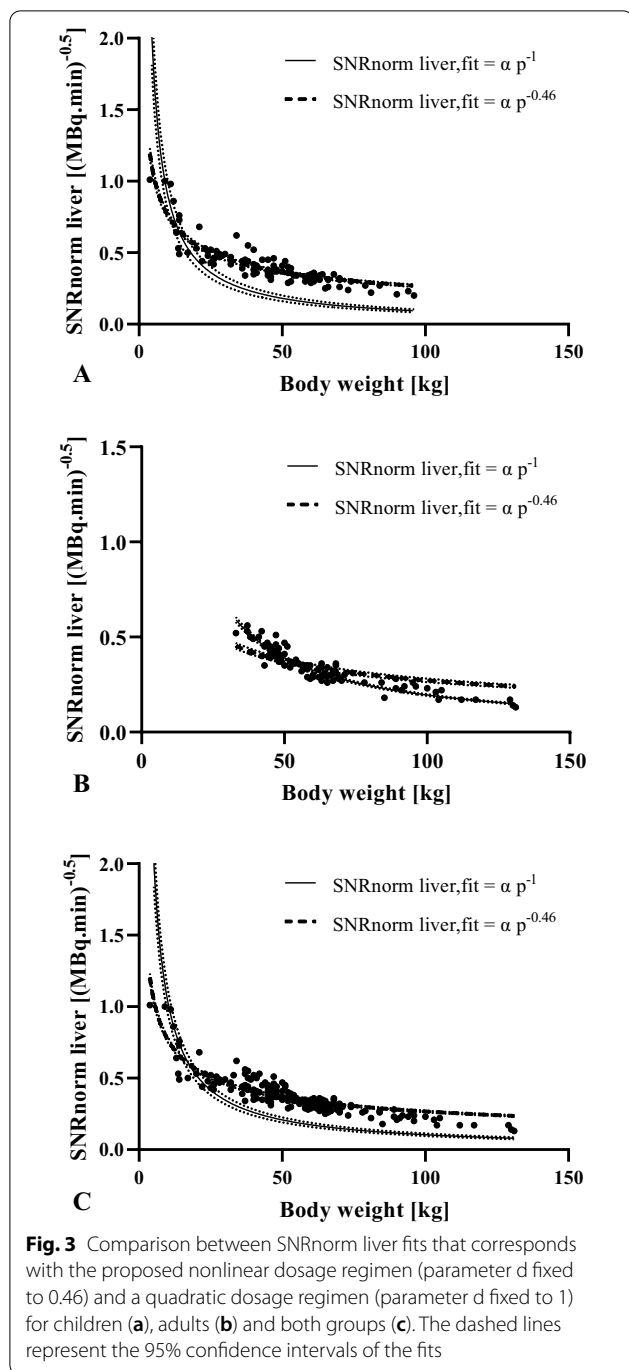
41% (NACG: 111 MBq and 6.2 mSv) and 63% (EANM: 178 MBq and 9.9 mSv) for a child of 30 kg, despite the higher amount of injected activity compared to the dosage regimen used in the current study (51 MBq and 2.9 mSv).

Discussion

In this study, the relation between patient-dependent parameters and [18F]FDG PET image quality was investigated in order to propose a dedicated paediatric dose regimen that aims for constant and sufficient image quality. To the best of our knowledge, this study is the first that investigates the relationship between paediatric patient-dependent parameters and [18F]FDG PET image quality based on SNR. This study has demonstrated that body weight is the parameter with the greatest effect on [18F]FDG image quality in children. Another important finding was that SNRnorm values were significant higher in children and correlated more strongly with age than in adults. Furthermore, this is the first study providing insight into the differences between paediatric and adult dosage regimens. This insight emphasizes the need for a dedicated paediatric dosage regimen, especially for young children.

Liver deoxyglucose metabolism in children was shown to be significantly lower than in adults. These results confirm the results obtained in a paediatric study by Yeung et al.[30]. The increase in [18F]FDG uptake during growth may be caused by age related changes in liver volume [34] and function of hepatocytes [35, 36]. Furthermore, the significant changes in body size, body composition [34, 37] and blood volume during growth [37] could also account for an increase in [18F]FDG uptake. Not only body size and age affected SUV measurements but also differences in uptake period, plasma glucose, recovery coefficient and partial volume artefacts [38]. The contribution of these factors may be limited in this study due to the use of standardized protocols.

Despite lower SUVbsa mean values and concomitant lower liver [18F]FDG uptake, small children showed high SNRnorm values, which implies that less activity is

Fig. 3 Comparison between SNRnorm liver fits that corresponds with the proposed nonlinear dosage regimen (parameter d fixed to 0.46) and a quadratic dosage regimen (parameter d fixed to 1) for children (**a**), adults (**b**) and both groups (**c**). The dashed lines represent the 95% confidence intervals of the fits

Fig. 4 Comparison of [^{18}F]FDG dosage regimens. Current study, EANM, NACG and the proposed dose regimen

needed to obtain sufficient image quality (Fig. 1a). This is probably caused by less attenuation and scatter due to the smaller body sizes. In contrast to SNRnorm, SNR has almost no correlation with age (Fig. 1b). This means that, despite the quite large spread (range 4.3–8.1), the currently used dosage regimen already provides a constant image quality throughout our patient population.
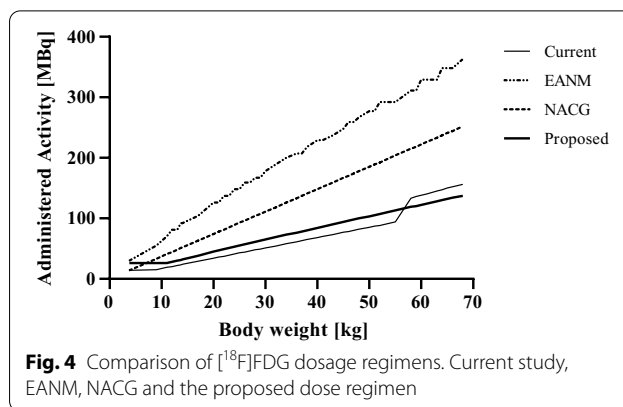
Body weight was the patient-dependent parameter with the highest coefficient of determination for both fit models for SNRnorm. The fit parameters ($\alpha = 2.23$ and $d = 0.46$) of the preferred model are in line with the fit parameters ($\alpha = 3.2$ and $d = 0.52$) obtained by van Gent et al. [21] in a paediatric pilot study of 20 patients. The fit of the preferred model was not significantly different from the fits of BMI, BWH and BSA, even though body mass was used to define the optimal dose regimen as it is more practical than BMI, BWH and BSA. Although the selected model explains 81% of variability in SNRnorm among patients, the remaining 19% was not explained. This variability might be caused by differences in patient size, not covered by body weight. Unknown inhomogeneities within the liver VOIs might also cause variability of SNRnorm. Nevertheless, our results are consistent with earlier adult [^{18}F]FDG studies of de Groot et al.[15] and Menezes et al.[39]. These studies determined body weight with the highest coefficient of determination with SNRnorm with, respectively, R^2's of 0.77 (OSEM 3D + PSF + TOF) and 0.86 (OSEM 3D + PSF) using comparable scanners to ours. Body weight was also identified as the best single predictor for image quality by Accorsi et al. [10] at a comparable R^2 of 0.86 using a different camera, reconstruction method and the noise equivalent count rate density (NECRD) as measure of image quality. The NECRD is derived from the noise equivalent count rate (NECR) method [19], which is considered to be more objectively related to SNR, since it is not affected by possible differences in liver metabolism and reconstruction methods [40–42]. However, at that moment NECRD was not validated with a visual assessment, and therefore, the estimated sufficient image quality and proposed dosage regimen could be unreliable [43].

In contrast to the studies mentioned above, this study directly compared the models of children and adults. It was not possible to find a universal dosing regimen linking paediatric and adult protocols (Fig. 3). This insight

Cox *et al. EJNMMI Res*   (2021) 11:65

Page 8 of 10

emphasizes the need for a dedicated paediatric dosage regimen, especially for young children. These results are in agreement with the EANM adult guidelines [14], which recommends using a quadratic dosage regimen, especially for patients > 75 kg, as this compensates for the lower image quality caused by substantial attenuation when using a linear dosage regimen [15]. In addition, they recommend that the linear dosage regimen is appropriate to use for patients < 75 kg, but this is not supported by data or references.

Our proposed paediatric [18F]FDG dosage regimen (acquisition time 3 mbp) showed a reduction of the amount of administered activity and effective dose of 41% (NACG) and 63% (EANM) in a child of 30 kg (Fig. 4). Our findings broadly support the work of other studies in this area, which also found reductions of 40–50% [10, 11, 22, 23], although they used other dosage regimens, scanners and reconstruction methods.

A limitation of our study is the absence of raw data due to the retrospective approach. Therefore, NECR analysis of the raw data to support the SNR data was not possible. The NECR data are more objective since they are not affected by differences in liver deoxyglucose metabolism and reconstruction parameters. An earlier adult study of Menezes et al. [39] determined that both SNR and NECR showed the best correlation with body weight. The clinical SNR analysis could be replicated in a phantom study by de Groot et al. [15] and this showed that the effects of liver glucose metabolism and reconstruction parameters are either rare or not as influential compared to attenuation effects. Another limitation is that we included only 85 adult patients against 102 children. However, we tried to create as much as possible equal patient distribution and adult patients below 55 kg and children above 95 kg are rare in our patient population. Furthermore, it should be pointed out that our study has been primary concerned with optimizing radiation dose from [18F]FDG rather than from both [18F]FDG and CT. The low-dose CT protocols of our scanners have already been optimized to reduce radiation dose (Child of 30 kg: DLP ± 75 mGy·cm and 1.4 mSv [44]) and to maintain sufficient image quality as with phantom studies in the past [26–28].

The results of this study are only valid for Siemens Biograph mCT scanners with an OSEM 3D + PSF + TOF reconstruction. However, the objective method applied in this study can be used for further investigation for other scanners and reconstruction methods to obtain evidence-based recommendations for different types of scanners in the guidelines. Recently, three paediatric PET/magnetic resonance imaging (PET/MR) studies concerning the newest generation large field of view PET scanners with solid-state silicon photomultipliers and higher TOF resolution showed already that even more dose reduction is possible due to their higher sensitivity [22, 45, 46], especially when MR replaces CT for localization and attenuation correction [47]. Another promising tool is the new block sequential regularized expectation maximization (BSREM/Q.Clear) reconstruction software [48–50] that generates images with higher image quality, which allows dose reduction. In the future, another step in dose reduction will be taken with the implementation of artificial intelligence (AI) technology in nuclear medicine imaging. AI technology offers a wide range of application opportunities for low-dose PET scans for example AI imaging [51, 52], AI reconstruction [53] and AI post-reconstruction image enhancement [54].

Conclusion

Body weight has the greatest effect on [18F]FDG PET image quality in children. The proposed nonlinear dosage regimen based on body mass will provide a constant and clinical sufficient image quality with a reasonable radiation dose and present a significant reduction of the administered activity compared to the current guidelines. A dedicated paediatric dosage regimen is necessary, as a universal dosing regimen for paediatric and adult is not feasible.

Abbreviations
18F-FDG: 18Fluorine-fluoro-2-deoxyglucose; PET/CT: Positron emission tomography/computed tomography; SNR: Signal-to-noise ratio; SNRnorm: Normalized signal-to-noise ratio; ALARA: As low as reasonably achievable; SNMMI: Society of Nuclear Medicine and Molecular Imaging; EANM: European Association of Nuclear medicine; NACG: North American Consensus guidelines; BW: Body weight; BMI: Body mass index; BWH: Body weight per body height; BSA: Body surface area; MBq/kg: Megabequerel per kilogram; OSEM: Ordered subset expectation maximization; PSF: Point spread function; TOF: Time of flight; VOI: Volume of interest; SD: Standard deviation; DTP: Dose–time product; AICc: Akaike's corrected information criterion values; ANOVA: Analysis of variance; NECRD: Noise equivalent count rate density; NECR: Noise equivalent count rate; PET/MR: Positron emission tomography/magnetic resonance imaging; BSREM: Block sequential regularized expectation maximization; AI: Artificial intelligence.

Declarations

Ethics approval and consent to participate
The study was approved by the Medical Ethical Committee of the Erasmus Medical Centre (reference number: 2021–0078).

Cox *et al. EJNMMI Res*   (2021) 11:65

Page 9 of 10

References

1. Masselli G, De Angelis C, Sollaku S, Casciani E, Gualdi G. PET/CT in pediatric oncology. Am J Nucl Med Mol Imaging. 2020;10(2):83.
2. Parisi MT, Otjen JP, Stanescu AL, Shulkin BL. Radionuclide imaging of infection and inflammation in children: a review. Semin Nucl Med. 2018;48(2):148–65.
3. Ozasa K, Shimizu Y, Suyama A, Kasagi F, Soda M, Grant EJ, et al. Studies of the mortality of atomic bomb survivors, Report 14, 1950–2003: an overview of cancer and noncancer diseases. Radiat Res. 2012;177(3):229–43.
4. ICRP. The 2007 recommendations of the international commission on radiological protection. ICRP publication 103. Ann ICRP. 2007;37(2–4): 2
5. WHO. Communicating radiation risks in Paediatric imaging. Geneva: WHO Press; 2016.
6. EANM. EANM Dosage Card (version 5.7.2016). https://www.eanm.org/docs/EANM_Dosage_Card_040214.pdf. Accessed:Aug 2016.
7. Vali R, Alessio A, Balza R, Borgwardt L, Bar-Sever Z, Czachowski M, et al. SNMMI procedure standard/EANM practice guideline on pediatric (18)F-FDG PET/CT for oncology 10. J Nucl Med. 2021;62(1):99–110.
8. Treves ST, Gelfand MJ, Fahey FH, Parisi MT. 2016 update of the North American consensus guidelines for pediatric administered radiopharmaceutical activities. J Nucl Med. 2016;57(12):15N-18N.
9. Alessio AM, Kinahan PE, Manchanda V, Ghioni V, Aldape L, Parisi MT. Weight-based, low-dose pediatric whole-body PET/CT protocols. J Nucl Med. 2009;50(10):1570–8.
10. Accorsi R, Karp JS, Surti S. Improved dose regimen in pediatric PET. J Nucl Med. 2010;51(2):293–300.
11. Alessio AM, Sammer M, Phillips GS, Manchanda V, Mohr BC, Parisi MT. Evaluation of optimal acquisition duration or injected activity for pediatric 18F-FDG PET/CT. J Nucl Med. 2011;52(7):1028–34.
12. Jacobs F, Thierens H, Piepsz A, Bacher K, Van de Wiele C, Ham H, et al. Optimised tracer-dependent dosage cards to obtain weight-independent effective doses. Eur J Nucl Med Mol Imaging. 2005;32(5):581–8.
13. Alkhybari EM, McEntee MF, Willowson KP, Brennan PC, Kitsos T, Kench PL. An Australian local diagnostic reference level for paediatric whole-body (18)F-FDG PET/CT. Br J Radiol. 2019;92(1096):20180879.
14. Boellaard R, Delgado-Bolton R, Oyen WJ, Giammarile F, Tatsch K, Eschner W, et al. FDG PET/CT: EANM procedure guidelines for tumour imaging: version 2.0. Eur J Nucl Med Mol Imaging. 2015;42(2):328–54.
15. de Groot EH, Post N, Boellaard R, Wagenaar NR, Willemsen AT, van Dalen JA. Optimized dose regimen for whole-body FDG-PET imaging. EJNMMI Res. 2013;3(1):63.
16. Halpern BS, Dahlbom M, Auerbach MA, Schiepers C, Fueger BJ, Weber WA, et al. Optimizing imaging protocols for overweight and obese patients: a lutetium orthosilicate PET/CT study. J Nucl Med. 2005;46(4):603–7.
17. Halpern BS, Dahlbom M, Quon A, Schiepers C, Waldherr C, Silverman DH, et al. Impact of patient weight and emission scan duration on PET/CT image quality and lesion detectability. J Nucl Med. 2004;45(5):797–801.
18. Masuda Y, Kondo C, Matsuo Y, Uetani M, Kusakabe K. Comparison of imaging protocols for 18F-FDG PET/CT in overweight patients: optimizing scan duration versus administered dose. J Nucl Med. 2009;50(6):844–8.
19. Watson CC, Casey ME, Bendriem B, Carney JP, Townsend DW, Eberl S, et al. Optimizing injected dose in clinical PET by accurately modeling the counting-rate response functions specific to individual patient scans. J Nucl Med. 2005;46(11):1825–34.
20. Geismar JH, Stolzmann P, Sah BR, Burger IA, Seifert B, Delso G, et al. Intra-individual comparison of PET/CT with different body weight-adapted FDG dosage regimens. Acta Radiol Open. 2015;4(2):1–9.
21. van Gent M, Hamming VC, Schaar JE, Glaudemans AWJM, Willemsen ATM. Dose optimization for pediatric FDG whole body PET/CT. Eur J Nucl Med Mol Imag. 2019;46(11):1.
22. Gatidis S, Schmidt H, la Fougere C, Nikolaou K, Schwenzer NF, Schafer JF. Defining optimal tracer activities in pediatric oncologic whole-body (18)F-FDG-PET/MRI. Eur J Nucl Med Mol Imaging. 2016;43(13):2283–9.
23. Kertesz H, Beyer T, London K, Saleh H, Chung D, Rausch I, et al. Reducing radiation exposure to paediatric patients undergoing [18F]FDG-PET/CT imaging. Mol Imaging Biol. 2021.
24. Lassmann M, Treves ST, Group ESPDHW. Paediatric radiopharmaceutical administration: harmonization of the 2007 EANM paediatric dosage card (version 1.5.2008) and the 2010 North American consensus guidelines. Eur J Nucl Med Mol Imaging. 2014;41(5):1036–41.
25. Du Bois D, Du Bois EF. A formula to estimate the approximate surface area if height and weight be known 1916. Nutrition. 1989;5(5):303–11.
26. Caan GA, Almeida AS, Segbers M. Phantom study into constant image quality of low-dose CT in the pediatric population. Eur J Nucl Med. 2014;41(10):2.
27. Caan GA, Almeida AS, Segbers M. Pediacrtic low-dose CT: how low can we go? Eur J Nucl Med. 2016;43(11):1.
28. Cox CPW, Segbers M., Straaten van M. Teenager: should one use a child or adult low dose computed tomography protocol?: https://epos.myesr.org/poster/esr/ecr2020/C-04435. Accessed Jul 2020.
29. Cox CPW, Segbers M, Graven LH, Brabander T, van Assema DME. Standardized image quality for (68)Ga-DOTA-TATE PET/CT. EJNMMI Res. 2020;10:27.
30. Yeung HW, Sanches A, Squire OD, Macapinlac HA, Larson SM, Erdi YE. Standardized uptake value in pediatric patients: an investigation to determine the optimum measurement parameter. Eur J Nucl Med Mol Imaging. 2002;29(1):61–6.
31. Schomburg A, Bender H, Reichel C, Sommer T, Ruhlmann J, Kozak B, et al. Standardized uptake values of fluorine-18 fluorodeoxyglucose: the value of different normalization procedures. Eur J Nucl Med. 1996;23(5):571–4.
32. Burnham KP, Anderson DR. Model selection and multimodel inference: A practical information-theoretic approach. 2nd ed. New York: Springer; 2002.
33. ICRP. Radiation Dose to Patients from Radiopharmaceuticals: a Compendium of Current Information Related to Frequently Used Substances. ICRP Publication 128. Ann ICRP. 2015;442:107–9.
34. Meier JM, Alavi A, Iruvuri S, Alzeair S, Parker R, Houseni M, et al. Assessment of age-related changes in abdominal organ structure and function with computed tomography and positron emission tomography. Semin Nucl Med. 2007;37(3):154–72.
35. Sastre J, Pallardó FV, Plá R, Pellín A, Juan G, O'Connor JE, et al. Aging of the liver: age-associated mitochondrial damage in intact hepatocytes. Hepatology. 1996;24(5):1199–205.
36. Grasedyck K, Jahnke M, Friedrich O, Schulz D, Lindner J. Aging of liver: morphological and biochemical changes. Mech Ageing Dev. 1980;14(3–4):435–42.
37. ICRP. Report of the task group on reference man. Ann ICRP. 1979;3(1–4).
38. Keyes JW Jr. SUV: standard uptake or silly useless value? J Nucl Med. 1995;36(10):1836–9.
39. Menezes VO, Machado MA, Queiroz CC, Souza SO, d'Errico F, Namias M, et al. Optimization of oncological (18)F-FDG PET/CT imaging based on a multiparameter analysis. Med Phys. 2016;43(2):930–8.
40. Wickham F, McMeekin H, Burniston M, McCool D, Pencharz D, Skillen A, et al. Patient-specific optimisation of administered activity and acquisition times for (18)F-FDG PET imaging. EJNMMI Res. 2017;7(1):3.
41. McDermott GM, Chowdhury FU, Scarsbrook AF. Evaluation of noise equivalent count parameters as indicators of adult whole-body FDG-PET image quality. Ann Nucl Med. 2013;27(9):855–61.
42. Mizuta T, Senda M, Okamura T, Kitamura K, Inaoka Y, Takahashi M, et al. NEC density and liver ROI S/N ratio for image quality control of whole-body FDG-PET scans: comparison with visual assessment. Mol Imaging Biol. 2009;11(6):480–6.
43. Watson CC. Injected dose in pediatric PET. J Nucl Med. 2010;51(10):1657.
44. ICRP. Managing Patient Dose in Multi-Detector Computed Tomography (MDCT). ICRP Publication 102. Ann ICRP. 2007;37(1):77.
45. Schmall JP, Surti S, Otero HJ, Servaes S, Karp JS, States LJ. Investigating low-dose image quality in whole-body pediatric ^{18}F-FDG scans using time-of-flight PET/MRI. J Nucl Med. 2021;62(1):123–30.

Cox *et al. EJNMMI Res*   (2021) 11:65

Page 10 of 10

46. Zucchetta P, Branchini M, Zorz A, Bodanza V, Cecchin D, Paiusco M, et al. Quantitative analysis of image metrics for reduced and standard dose pediatric (18)F-FDG PET/MRI examinations. Br J Radiol. 2019;92(1095):20180438.

47. Gatidis S, Schmidt H, Gucke B, Bezrukov I, Seitz G, Ebinger M, et al. Comprehensive oncologic imaging in infants and preschool children with substantially reduced radiation exposure using combined simultaneous (1)(8)F-fluorodeoxyglucose positron emission tomography/magnetic resonance imaging: a direct comparison to (1)(8)F-fluorodeoxyglucose positron emission tomography/computed tomography. Invest Radiol. 2016;51(1):7–14.

48. Lindstrom E, Sundin A, Trampal C, Lindsjo L, Ilan E, Danfors T, et al. Evaluation of penalized-likelihood estimation reconstruction on a digital time-of-flight PET/CT scanner for (18)F-FDG whole-body examinations. J Nucl Med. 2018;59(7):1152–8.

49. Parvizi N, Franklin JM, McGowan DR, Teoh EJ, Bradley KM, Gleeson FV. Does a novel penalized likelihood reconstruction of 18F-FDG PET-CT improve signal-to-background in colorectal liver metastases? Eur J Radiol. 2015;84(10):1873–8.

50. Tragardh E, Minarik D, Almquist H, Bitzen U, Garpered S, Hvittfelt E, et al. Impact of acquisition time and penalizing factor in a block-sequential regularized expectation maximization reconstruction algorithm on a Si-photomultiplier-based PET-CT system for (18)F-FDG. EJNMMI Res. 2019;9(1):64.

51. Hu Z, Li Y, Zou S, Xue H, Sang Z, Liu X, et al. Obtaining PET/CT images from non-attenuation corrected PET images in a single PET system using Wasserstein generative adversarial networks. Phys Med Biol. 2020;65(21):215010.

52. Sanaat A, Shiri I, Arabi H, Mainta I, Nkoulou R, Zaidi H. Deep learning-assisted ultra-fast/low-dose whole-body PET/CT imaging. Eur J Nucl Med Mol Imaging. 2021.

53. Wang YJ, Baratto L, Hawk KE, Theruvath AJ, Pribnow A, Thakor AS, et al. Artificial intelligence enables whole-body positron emission tomography scans with minimal radiation exposure. Eur J Nucl Med Mol Imaging. 2021.

54. Katsari K, Penna D, Arena V, Polverari G, Ianniello A, Italiano D, et al. Artificial intelligence for reduced dose 18F-FDG PET examinations: a real-world deployment through a standardized framework and business case assessment. EJNMMI Phys. 2021;8(1):25.

Publisher's Note